HOPE CREEK GENERATING STATION
FACILITY OPERATING LICENSE NPF-57
DOCKET NO. 50-354

REQUEST FOR LICENSE AMENDMENT
EXTENDED POWER UPRATE

Stress Analysis of the Hope Creek Unit 1 Steam Dryer for CLTP
CDI Report No. 06-24, Revision 3
September 2006

C.D.I. Report No. 06-24

Stress Analysis of the Hope Creek Unit 1 Steam Dryer for CLTP

Revision 3

Prepared by

Continuum Dynamics, Inc.
34 Lexington Avenue
Ewing, NJ 08618

Prepared under Purchase Order No. 4500341046 for

Nuclear Business Unit, PSEG Nuclear LLC
Materials Center, Alloway Creek Neck Road
Hancocks Bridge, NJ 08038

Approved by

Alan J. Bilanin

Reviewed by

Alexander H. Boschitsch

September 2006

Executive Summary

In this analysis, stresses induced by the flow of steam through the steam dryer at Hope Creek Unit 1 are calculated and evaluated at Current Licensed Thermal Power (CLTP). The fluctuating pressure loads induced by the flowing steam were predicted by a separate acoustic circuit analysis of the steam dome and main steam lines. These loads are applied to the steam dryer structure at 300 time steps with 0.002 sec interval for total of 0.6 sec. The resulting stresses are calculated by performing a time history structural dynamics analysis using the commercial finite element model, ANSYS 10.0.

Assessment of the stress results for compliance with the ASME B&PV Code, Section III, subsection NG, has been carried out for the load combination for normal operation (the Level A Service Condition). This combination consists almost entirely of the fluctuating pressure loads and weight. Evaluation is done for maximum stress, as well as for cyclic (fatigue type) stress. Level B service conditions, which include seismic loads, are not included in this evaluation.

The results for the Level A service condition show that there are locations with stresses comparable to the allowable values, with a minimum stress ratio of 1.54 (stress ratio is the allowable stress divided by the calculated stress). Stress ratios for specific locations on the steam dryer are tabulated in the report. It is emphasized that no additional adjustments associated with modeling uncertainty, correlations with plant data and in-plant conservatism are reflected in these stress ratios. Accounting for these adjustments is expected to further increase the stress ratios so that CLTP operational stresses are expected to be well within allowable levels.

This analysis includes all Hope Creek Unit 1 dryer modifications and accounts for the current power generation rate. To evaluate additional dryer modifications and/or power uprates, the stresses should be recomputed using appropriately modified structural models to account for steam dryer modifications, and main steam line strain gage measurements taken during power uprate and processed by a separate acoustic circuit analysis.

Table of Contents

Section Page

1. Introduction and Purpose

Recent inspections of the steam dryers in Mark I plants have shown cracks in the fillet welds and nearby structures. The industry has addressed this problem with physical modifications to the dryers, as well as a program to define steam dryer loads and their resulting stresses.

Hope Creek Unit 1 (HC1) is part of this program. The purpose of the stress analysis discussed here is to calculate stresses from the anticipated steam dryer loads at HC1 and compare those stresses to acceptance criteria from the ASME Code. This step will ensure that the modifications are adequate and that future weld cracking will not occur.

The damaging steam dryer loads are due to pressure fluctuations, induced by steam flow through the dryer. Over a long period of time, cyclic stresses from these loads can produce fatigue cracking if loads are sufficiently high. Since fillet welds are the structural features most susceptible to fatigue failure, most of the failures have been found in these areas.

The fluctuating pressure loads, induced by the flowing steam, were previously predicted by a separate acoustic circuit analysis of the steam dome and main steam lines [1]. In the present analysis, these loads are applied to the steam dryer structure and the resulting stresses calculated using a finite element model (the ANSYS 10.0 computer code). The loads are applied to the structure at 300 time steps with 0.002 sec interval for total 0.6 sec, and the equations representing the structural dynamics solved using a time history dynamic analysis.

The load combination considered here corresponds to normal operation (the Level A Service Condition) and consists almost entirely of the fluctuating pressure loads and weight. The resulting stresses are examined for compliance with the ASME B&PV Code, Section III, subsection NG. Both maximum and cyclic (fatigue type) stresses are considered in this evaluation. Level B service conditions, which include seismic, are not addressed.

2. Model Description

A description of the ANSYS model of the HC1 steam dryer follows.

2.1 Steam Dryer Geometry

A geometry model of the HC1 steam dryer was developed from available drawings, as well as from field measurements taken by C.D.I. on an identical spare dryer for the cancelled Hope Creek Unit 2. The completed model is shown in Figure 2.1.

This model includes modifications made to the HC1 steam dryer on-site, prior to commercial operation. These are:

- Tie bars, hoods, and end plates were replaced on the original dryer (FDI-041-79450)
- Reinforcement bars were added to the hoods (FDDR-KT1-415 and KT1-444)

The modified areas are shown in Figure 2.2.

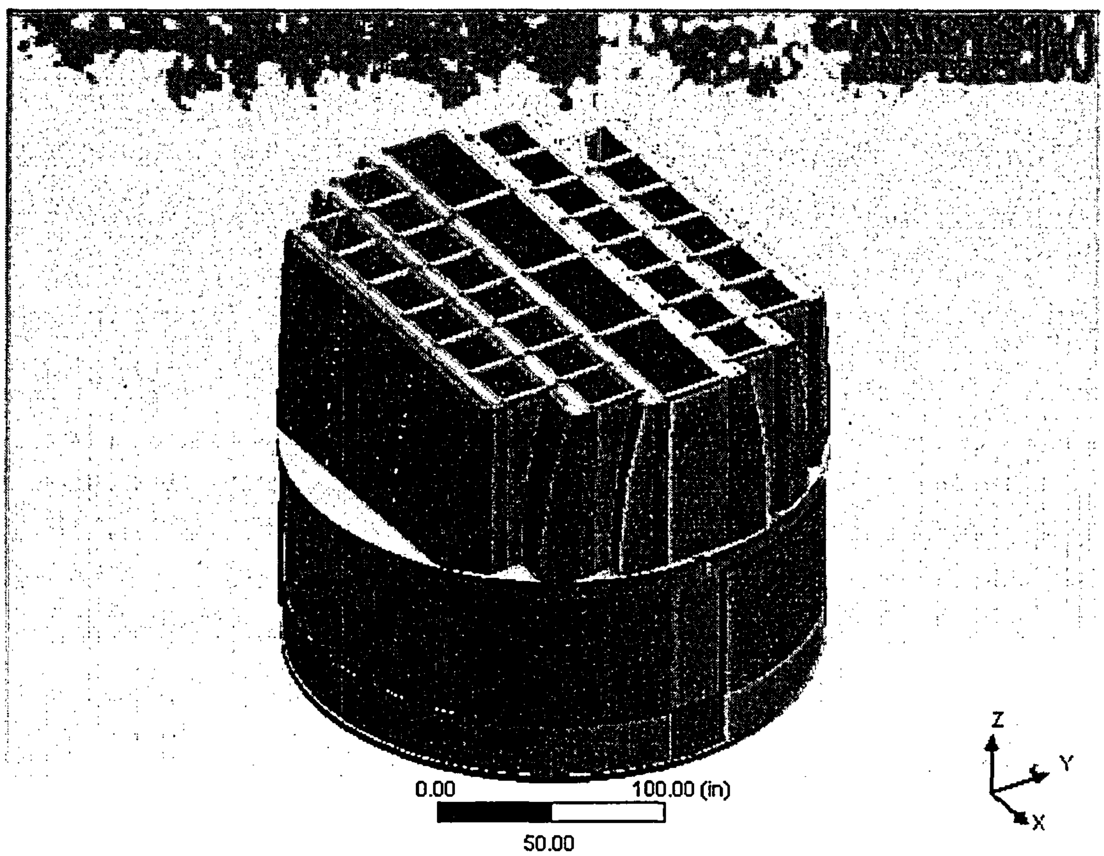

Figure 2.1. Overall geometry of the HC1 steam dryer model.

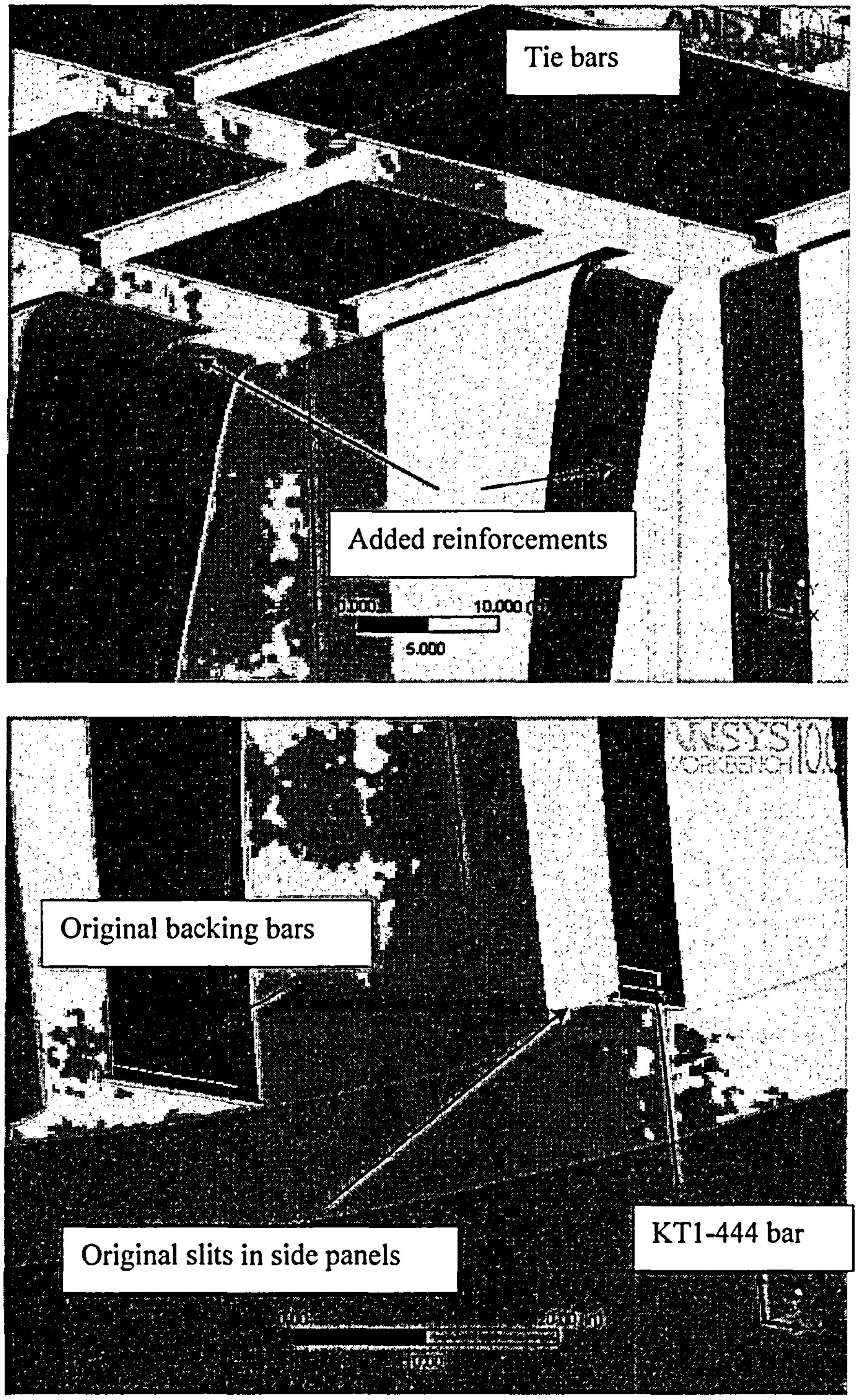

Figure 2.2. On-site modifications accounted for in the model and associated geometrical details.

2.2 Material Properties

The steam dryer is constructed from Type 304 stainless steel and has an operating temperature of 550°F. Properties used in the analysis are summarized in Table 2.1.

Table 2.1. Material properties.

	Young's Modulus (10^6 psi)	Density (lbm/in^3)	Poisson Ratio
Structural Steel	25.55	0.284	0.3
Structural Steel for Perforated Plates	15.33	0.227	0.3
Structural Steel with Added Water Inertia Effect	25.55	1.183	0.3

The structural steel modulus is taken from Appendix A of the ASME Code for Type 304 Stainless Steel at an operating temperature 550°F. The effective properties of perforated plates and submerged parts are discussed in Section III.

2.3 Pressure Loading

The transient loads are produced by the unsteady pressures acting on the exposed surfaces of steam dryer. The pressure time history loading was obtained from an acoustic circuit model of the HC1 steam dryer, performed by C.D.I. and detailed in [1]. The unsteady pressure loads applied to the dryer contain a strong 80Hz component which is not present in the plant. The erroneous signal was artificially introduced because of random noise in the sensors on the MSLs [3]. The stress assessment was therefore performed with the 80Hz signal removed. This loading was provided over the steam dryer surface on a three-inch grid, at a total of 10,963 locations. The time interval spanned the 0.6 sec of data that contained the peak minimum and maximum pressures on a low-resolution grid of the dryer (including only corners and edges, a total of 104 locations).

These results were interpolated onto the detailed structural grid of the HC1 steam dryer, and the ANSYS calculation was then undertaken. The program was developed to properly convert the data into a format recognizable by the ANSYS software. Inspection of the resulting pressures at selected nodes shows that these pressures vary in a well-behaved manner between the nodes with prescribed pressures. Graphical depictions of the resulting pressures, comparisons between the peak pressures in the original nodal histories and those in the final surface load distributions produced in ANSYS, and comparison of the pressure histories at randomly selected nodes in the original pressure history data files and the ANSYS loading arrays, all confirm that the load data is interpolated accurately and transferred correctly to ANSYS.

The fluctuating pressure loads were applied to surfaces above the water level, as indicated in Figure 2.3. In addition to the fluctuating pressure load, the static loading by the weight of the steam dryer is analyzed separately. The resulting static and transient stresses are linearly combined to obtain total values which are then processed to calculate peak and alternating stress intensities for assessment in Section 4.

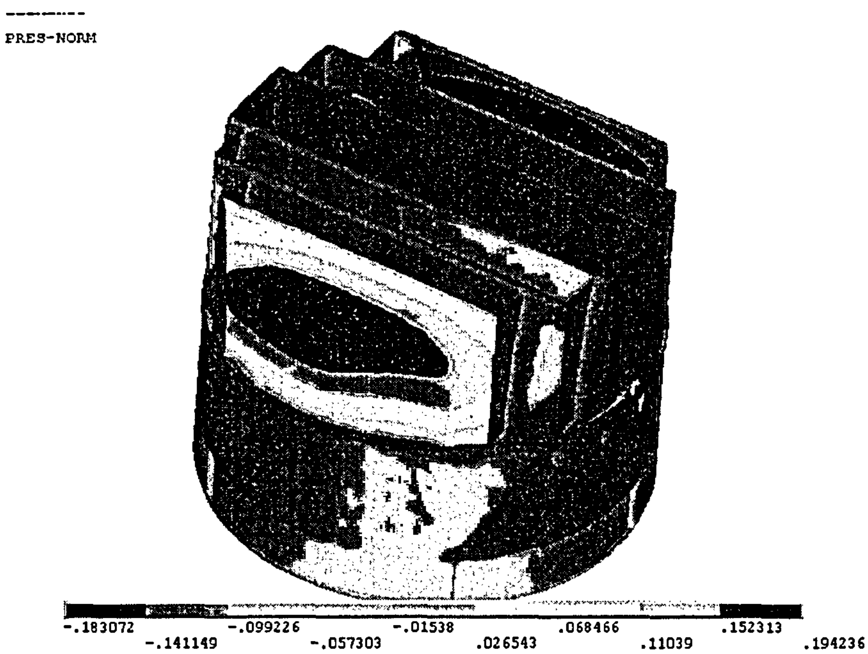

Figure 2.3. Typical pressure loading (in psid) on the steam dryer.

3.0 Finite Element Model

The dynamics of the steam dryer were modeled using the ANSYS computer code.

3.1 Model Simplifications

The following simplifications were made in order to reduce model size and retain key structural properties:

- Welds were mostly replaced by node-to-node connections; interconnected parts share the common nodes along the welds. In other locations the contact element technology, provided by ANSYS, was used, namely, bonded contact was established between connected parts.

- The drying vanes were replaced by point masses, attached to the corresponding base plates and vane bank top covers (Figure 3.1). The bounding perforated plates, vane banks, and vane covers were explicitly modeled.

- The lower part of the skirt and drain channels are below the reactor water level. An analysis was used to calculate the effective mass of this water and thus account for its interaction with the structure. This added water mass was included in the ANSYS model by appropriately modifying the density of the submerged structural elements when computing transient loads.

- Fixed constraints were imposed at the underside of the steam dryer upper support ring where it makes contact with the four steam dryer support brackets that are located on the reactor vessel and spaced at 90° intervals (Figure 3.2). No credit was taken for the constraints from the reactor vessel lift lugs.

3.2 Perforated Plate Model

The perforated plates were modeled as solid plates with adjusted elastic and dynamic properties. Properties of the perforated plates were assigned according to the type and size of perforation. Based on [2], for an equilateral triangular pattern with given hole size and spacing the effective modulus of elasticity was found to be a factor of 0.6 times the original modulus, while the effective density was a factor of 0.8 times the original steel density. These adjusted properties were shown in Table 2.1.

3.3 Vane Bank Model

The vanes were modeled as point masses, located at the center of mass for each vane bank. The following approximate masses were used for the vanes, based on data found on drawings supplied by PSE&G: inner banks, 6,500 lbm; middle banks, 5,900 lbm; and outer banks, 4,600 lbm. These weights were applied to the base plates and vane top covers using the standard ANSYS point mass modeling option, element MASS21. ANSYS automatically distributes the point mass inertial loads to the nodes of the selected structure. The distribution algorithm minimizes the sum of the squares of the nodal inertial forces, while ensuring that the net forces and moments are conserved. Vane banks are not exposed to main steam lines directly, but rather shielded by the hoods. Thus, compared to the hoods, less motion is anticipated on the vane banks so that approximating their inertial properties with equivalent point masses is justified. Nevertheless, the bounding parts, such as perforated plates, side panels and top covers are retained in the model.

3.4 Water Inertia Effect on Submerged Panels

Water inertia was modeled by an increase in density of the submerged structure. The added mass was found by a separate analysis to be 0.225 lbm/in^2 of submerged skirt area.

3.5 Structural Damping

Time history analysis in the ANSYS program requires that the damping be specified in terms of mass and stiffness Raleigh damping (i.e., the damping parameters, α and β, defined in Section 5.9.3 of the ANSYS 10.0 documentation). These material constants can be defined from the damping ratio over the range of frequencies examined. For the calculation presented here, a damping ratio of 1% was assumed over the range of frequencies from 10 to 150 Hz. This assumption leads to the following values used in the analysis: $\alpha = 1.18$ and $\beta = 2 \times 10^{-5}$. This damping is consistent with guidance given in NUREG-1.61.

3.6. Mesh Details and Element Types

Shell elements were employed to model the skirt, drain channels, hoods, perforated plates, side and end panels, trough bottom plates, reinforcements and cover plates. Specifically, the four-node, linear shell elements (triangles and quadrilaterals), that are the default shell element types recommended in ANSYS, were used. All other parts, including tie bars and the upper and lower support rings, were modeled with solid elements.

Most connections between parts were modeled as node-to-node connections. However, in several places, such as connections between shell and solid elements or dissimilarly meshed parts, the bonded contacts featured in ANSYS, were used. Bonded contacts impose penalty-based constraints on the close-proximity nodes, such that the relative motion is restricted by a high stiffness factor. The stiffness of such bonds is much higher than the structural stiffness, thus providing an effective model for interconnected parts. The structural model was refined to ensure proper operation of bonded contacts (the recommended way of assembling large complex structures in ANSYS) and achieve adequate mesh density.

Mesh details and element types are shown in Tables 3.1 and 3.2. The mesh was refined at locations such as curved regions on the hoods and drains channels, tie bars, the upper and bottom support rings and locations of high static stresses. Typical examples are shown in Figures 3.3 to 3.7.

Mesh sensitivity of the model was studied using static calculations of the structure subjected only to its own weight, see Section 4.1.

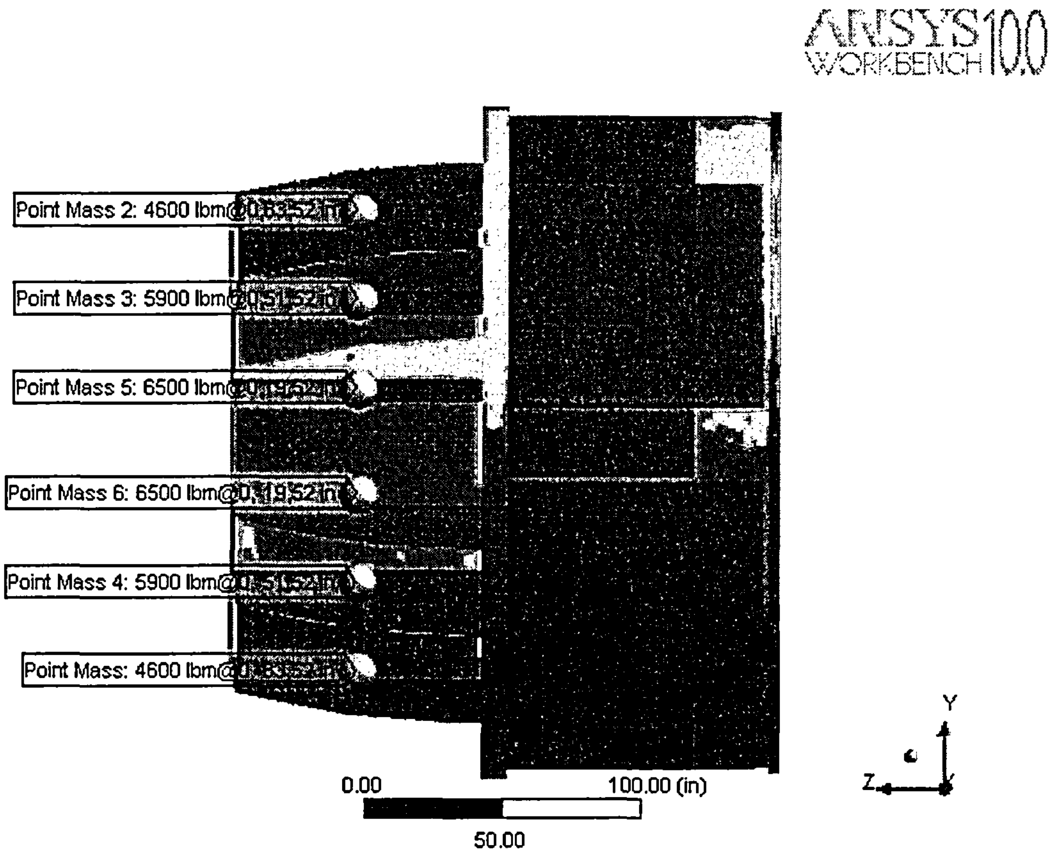

Figure 3.1. Point masses replaced the vanes.

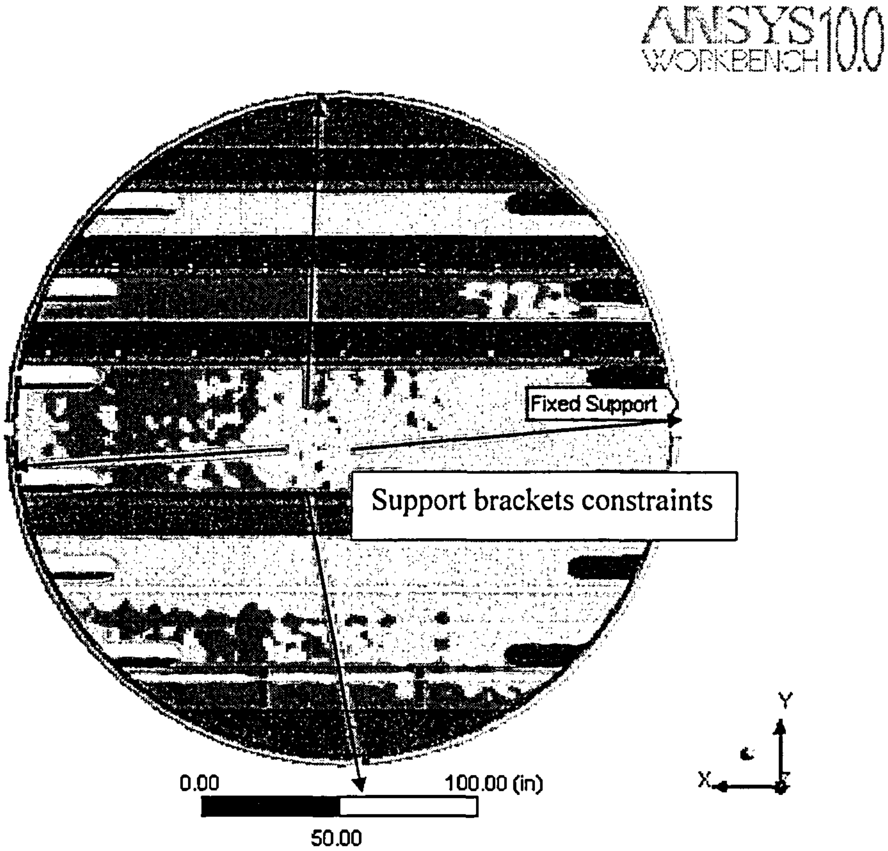

Figure 3.2. Fixed support constraints.

Table 3.1. FE Model Summary.

Description	Quantity
Total Nodes	85,135
Total Structural Elements	72,028
Element Types	10
Materials	3

Table 3.2 Listing of Element Types.

Generic Element Type Name	Element Name	ANSYS Name
10-Node Quadratic Tetrahedron	Solid187	10-Node Tetrahedral Structural Solid
20-Node Quadratic Hexahedron	Solid186	20-Node Hexahedral Structural Solid
4-Node Linear Triangular Shell	Shell181	4-Node Structural Shell
4-Node Linear Quadrilateral Shell	Shell181	4-Node Structural Shell
Quadratic Quadrilateral Contact	Conta174	High-Order Surface to Surface Contact
Linear Quadrilateral Target	Targe170	Surface Contact Target
Linear Triangular Contact	Conta173	Low-Order Surface to Surface Contact
Linear Triangular Target	Targe170	Surface Contact Target
Mass Element	Mass21	Structural Mass
Pressure Surface Definition	Surf154	3D Structural Surface Effect

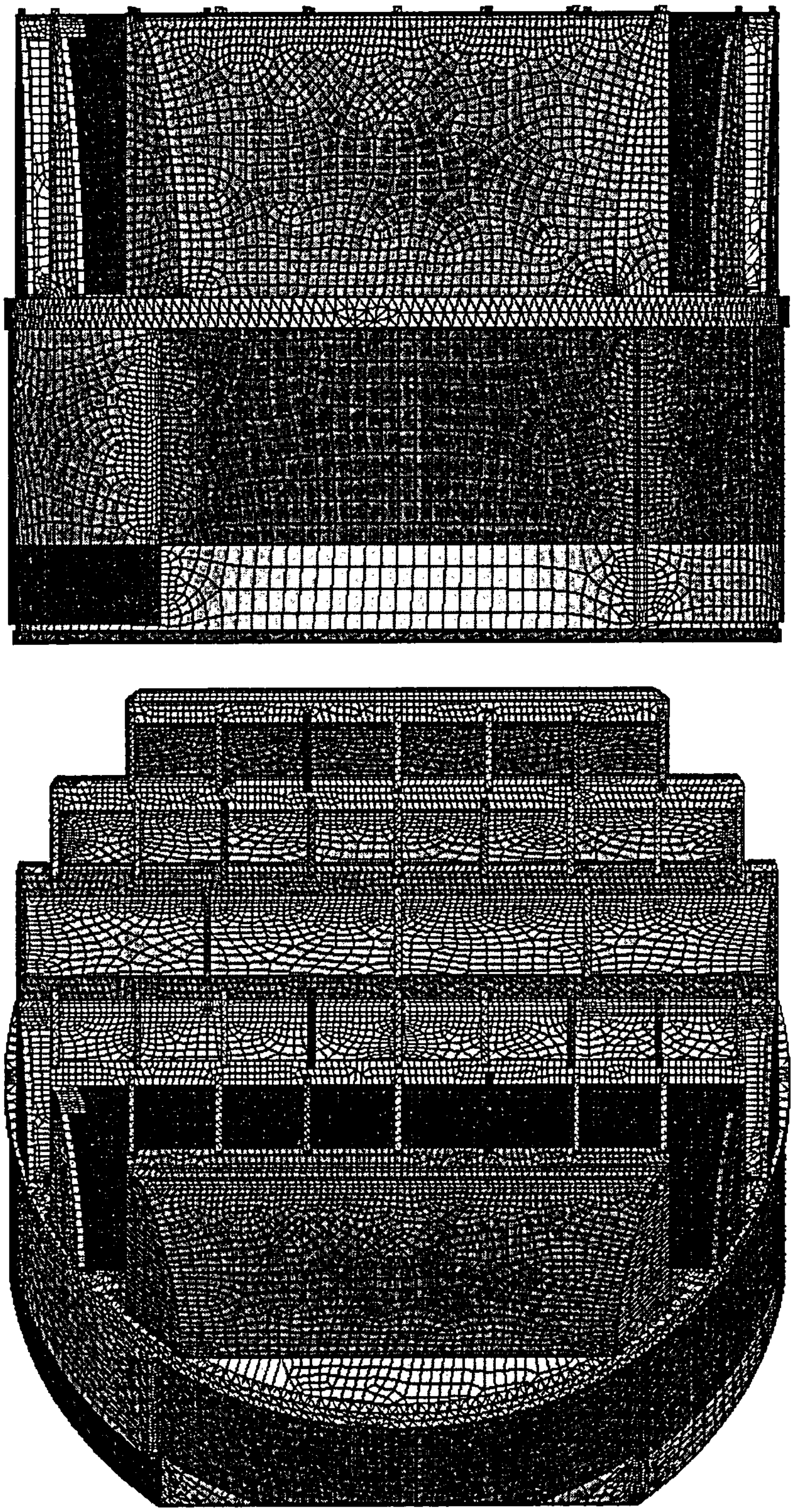

Figure 3.3. Mesh overview. The colors emphasize element type.

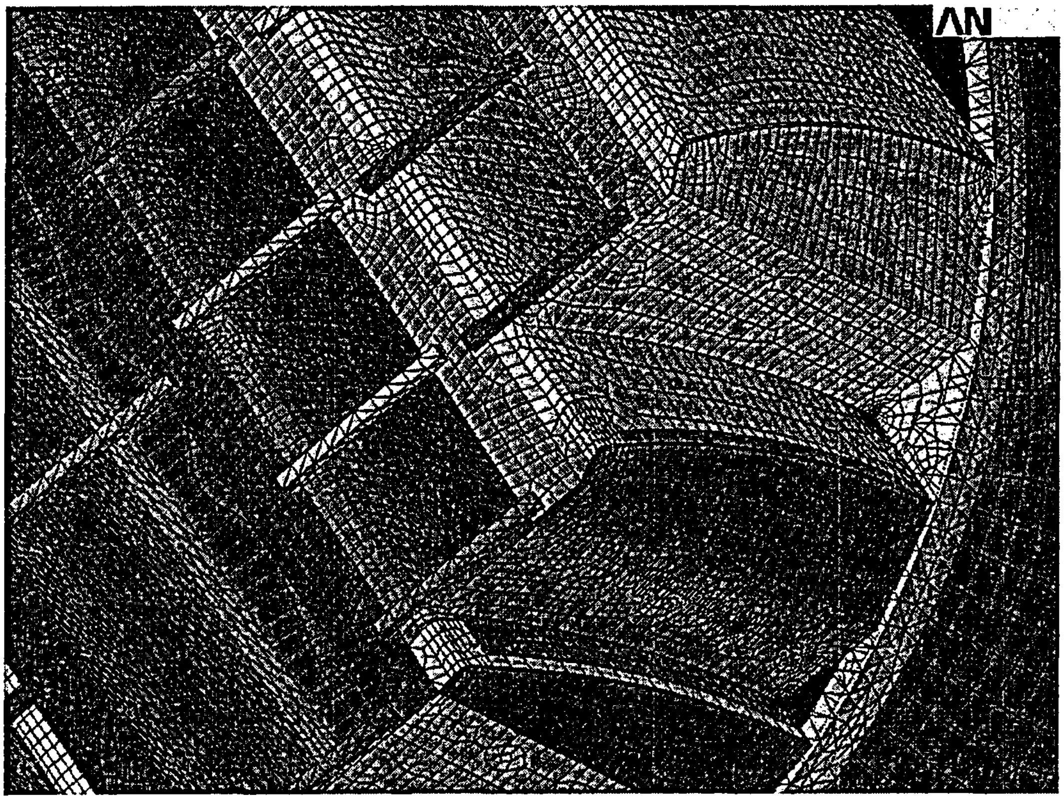

Figure 3.4. Close up of mesh showing hoods, reinforcement panels and tie bars. The colors emphasize element type.

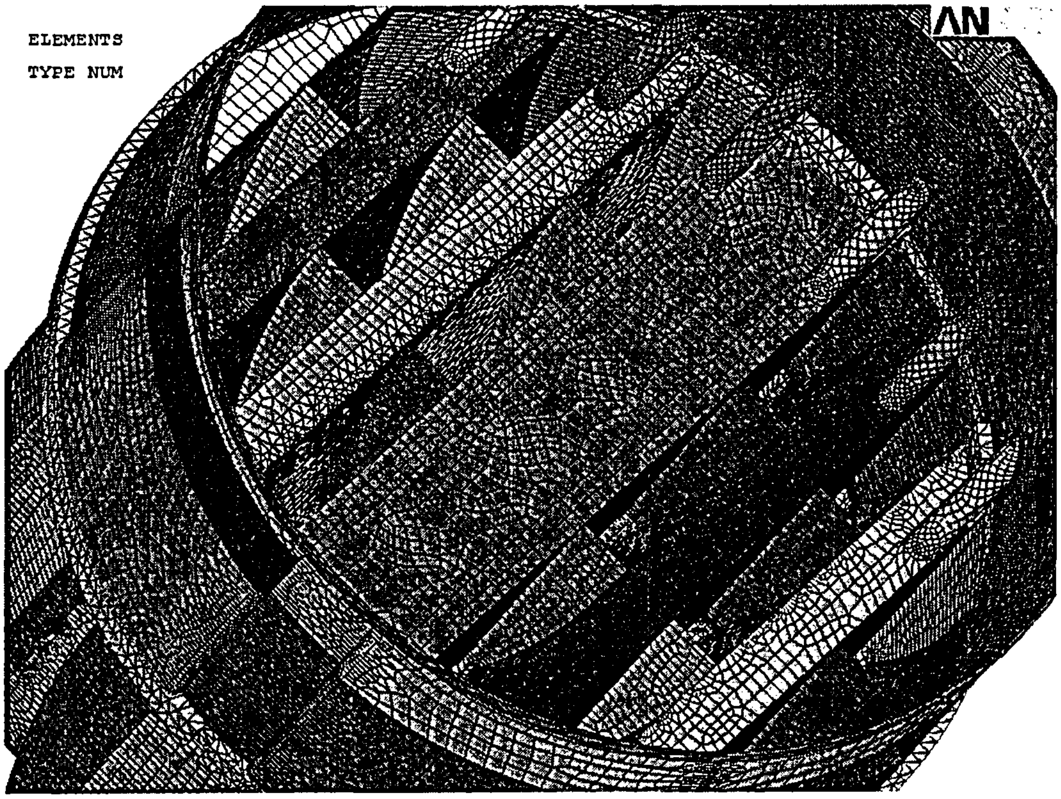

Figure 3.5. Close up of mesh showing drain pipes and hood supports. The colors emphasize element type.

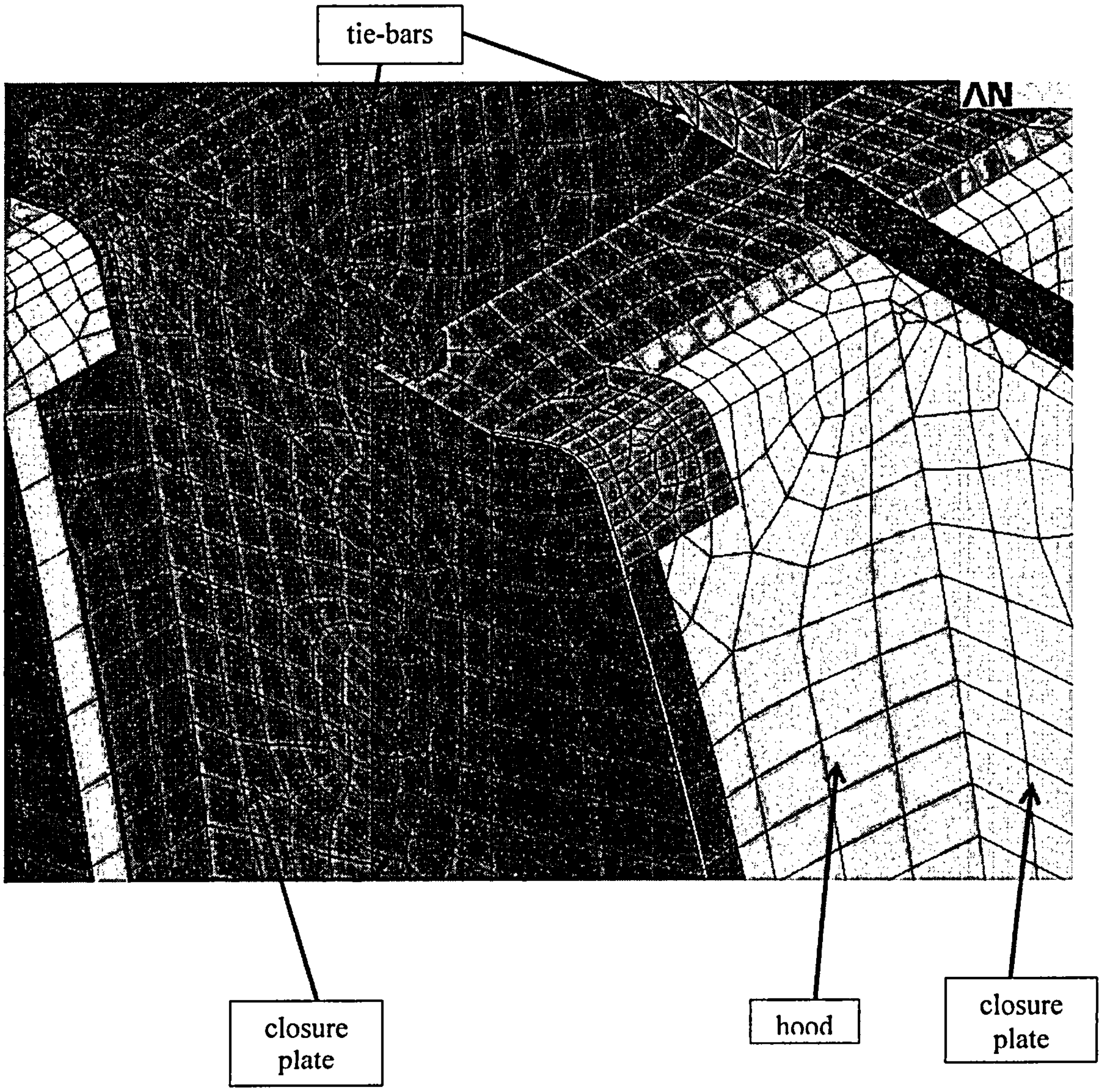

Figure 3.6. Close up of mesh showing node-to-node connections between closure panels, end plates, and hoods. Bonded contacts are used for tie bars and hood reinforcements. The colors emphasize element types.

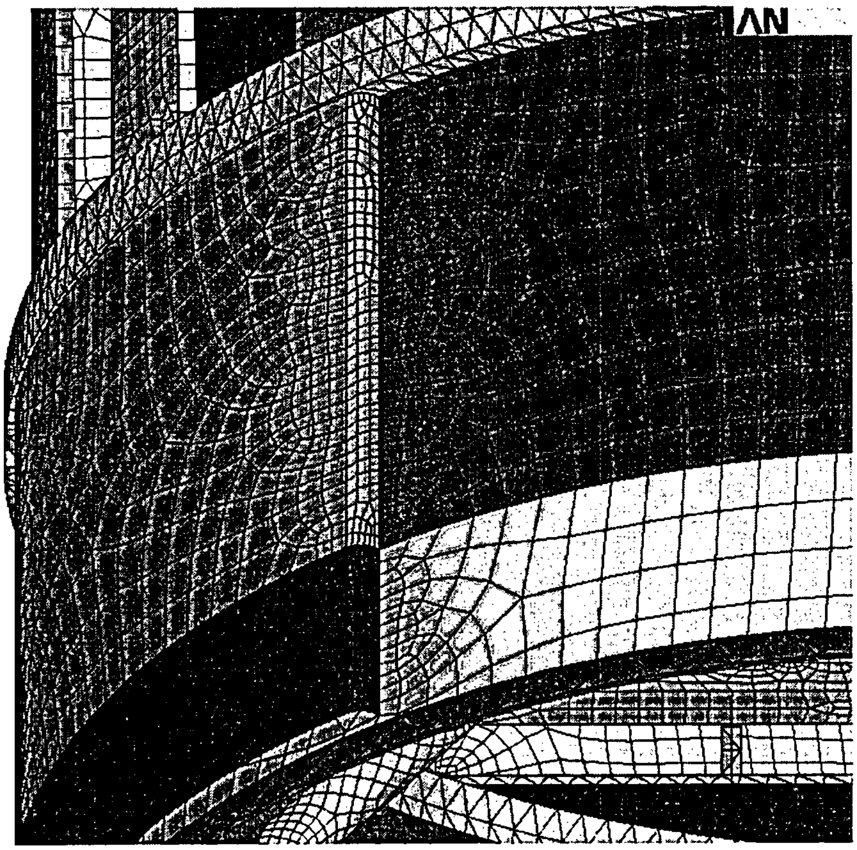

Figure 3.7. Close up of mesh showing node-to-node connections between the skirt and drain channels. Bonded contacts are used for the upper and lower support rings. The colors emphasize element type.

4. Structural Analysis

The solution is decomposed into static and transient parts. The static solution produces the stress field induced by the supported structure subjected to its own weight, whereas the transient solution accounts for the unsteady stress field due to the acoustic loads acting on the dryer. The two solutions are linearly combined to obtain the final displacement and stress histories. This decomposition facilitates prescription of the added mass model accounting for hydrodynamic interaction and allows one to compare the stress contributions arising from static and unsteady loads separately.

4.1 Static Analysis

The results of the static analysis are shown on Figure 4.1. Only a few locations exhibited high stress intensity levels. These locations include the trough thin section/thick closure plate/vane bank end plate junction with stress intensity 6,387 psi and the thin closure plate/inner hood junction with stress intensity 5,956 psi. Both locations are above one of the steam dryer support brackets.

The highest stresses are localized and full resolution of these small features would require enormous numerical effort. However, in the calculations on the present mesh, the stresses in these locations are found to be close to more refined mesh calculations.

Because of the model complexity and the fact that refinements are performed selectively in those regions identified by ANSYS as having higher error, the convergence with grid count is not uniform. The peak *transient* stresses occur away from structural junctions or supports and thus converge more rapidly with mesh density than the stress fields near structural junctions. Most of the lowest stress ratios (Table 6.3) occur at welds where the stress concentration effects are already implicitly accounted for by the factors of 0.55 (reduction in allowable stress) or 1.8 (increase in computed stress). The remaining high stresses occurring at non-weld locations in Table 6.3 are located away from structural junctions. Hence, they converge more rapidly with mesh density than the stress fields near structural junctions.

The locations with high static stress intensity are shown in Figure 4.2. Note that both locations have high stress intensity also when static and transient runs are combined, primarily due to static loading.

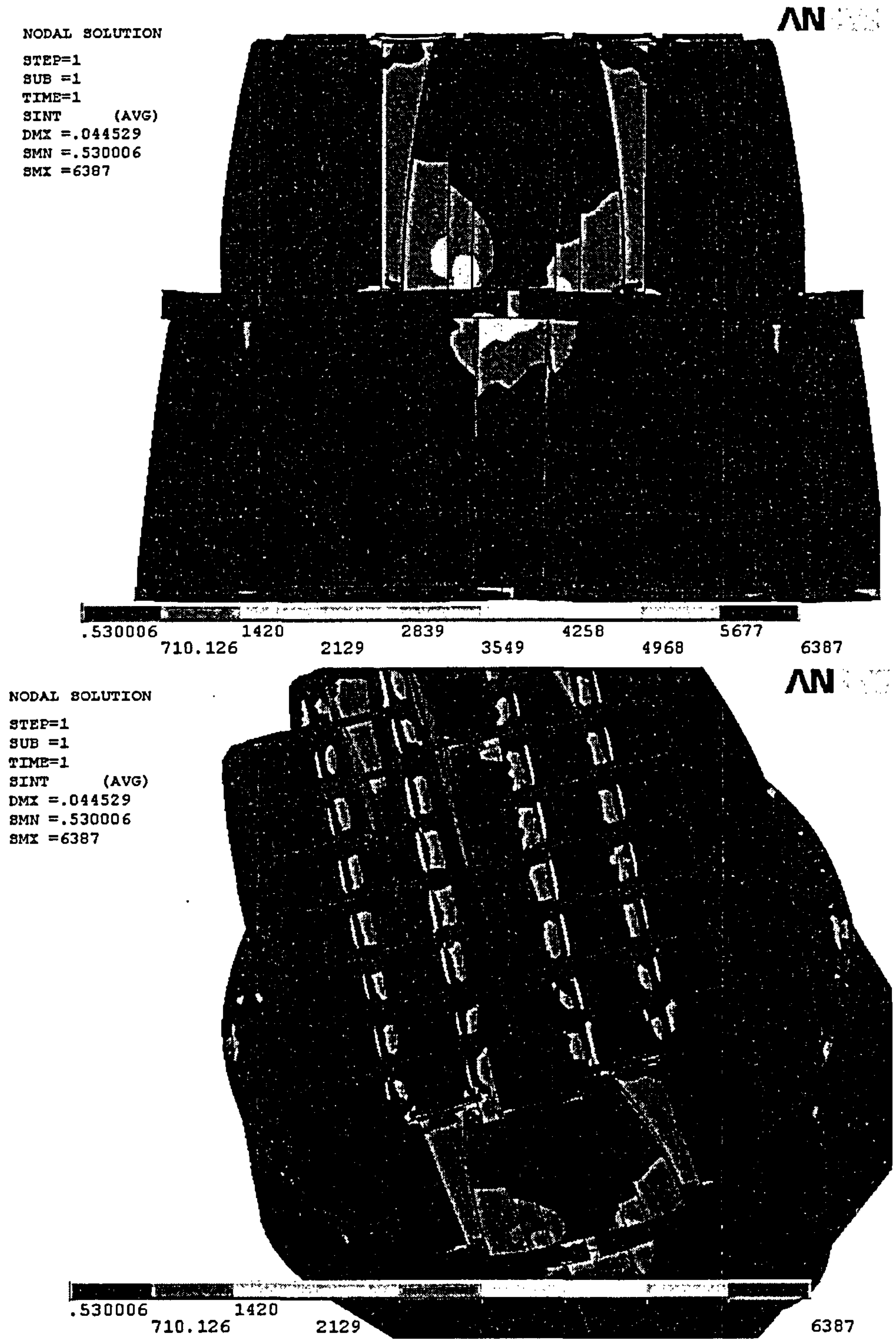

Figure 4.1. Overview of static calculations showing stress intensities (in psi) and displacements. Maximum displacement (DMX) is 0.045"; maximum stress intensity (SMX) is 6,387 psi.

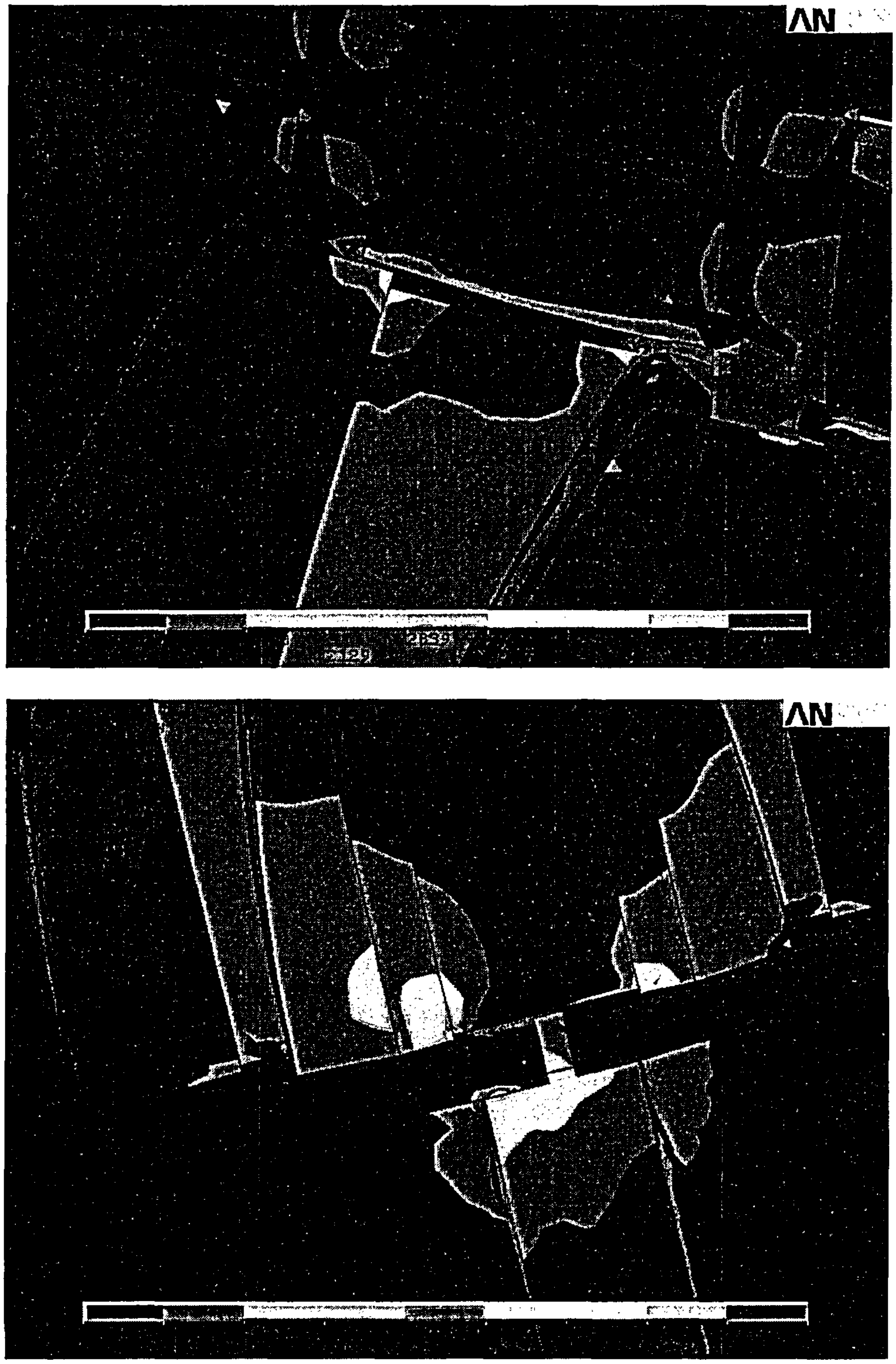

Figure 4.2. Close up of high static stress intensity (in psi) locations at closure plates and near support brackets.

4.2 Transient analysis

The fluctuating pressure loads were applied to the structural model at all surface nodes described in Section 2.3. The pressures were varied at increments of 0.002 sec for 300 time steps – a total time of 0.6 sec. These stress results are discussed in Section 5.

Stresses were calculated for each time increment, and a post-processor was used to combine results from static and transient calculations, to determine the maximum stress times, the stress intensities at these time points, and the alternating stress intensities over the time history. These stress intensities are then used in the evaluation in Section 5.

According to ASME B&PV Code, Section III, Subsection NG-3216.2 the following procedure was established to calculate alternating stresses. For every node, the stress difference tensors, $\sigma'_{nm} = \sigma_n - \sigma_m$, were considered for all possible pairs of the stresses σ_n and σ_m at different time steps, t_n and t_m. Note that all possible pairs require consideration since there are no 'obvious' extrema in the stress responses. For each stress difference tensor, the principal stresses S_1, S_2, S_3 were computed and the maximum absolute value among principal stress differences, $S_{nm} = \max\{|S_1 - S_2|, |S_1 - S_3|, |S_2 - S_3|\}$, obtained. The alternating stress at the node was then one half the maximum value of S_{nm} taken over all combinations (n,m), i.e., $S_{alt} = \frac{1}{2}\max_{n,m}\{S_{nm}\}$. This alternating stress was compared against allowable values, depending on the node location with respect to welds.

The peak stress was defined for each node as the largest stress intensity occurring during the time history. For shell elements the peak stresses were calculated separately at the mid-plane, where only membrane stress is present, and at top/bottom of the shell, where bending stresses are also present. The calculated values are compared against allowable values corresponding to stress category, Pm for membrane stress, and Pm + Pb for combined membrane and bending stress. For solid elements the peak stresses the most conservative allowable, Pm for membrane stress, was used, although the bending stress almost always is present in solid elements. Node location with respect to welds is also taken into account.

The peak stresses were compared against allowables values which depend upon the stress type (membrane, membrane+bending, alternating – Pm, Pm+Pb, S_{alt}) and location (at a weld or away from welds). The structure is then assessed in terms of stress ratios formed by dividing allowables by the computed stresses at every node. Stress ratios less than unity imply that the associated peak and/or alternating stress intensities exceed the allowable levels. Post-processing tools calculate the stress ratios and identify nodes with low stress ratios.

5. Results

5.1 General Stress Distribution

The ANSYS program provides contour plots of stress intensity based on smoothing of the nodal values over the surface. Typical contour plots, demonstrating stress intensity distribution over the structure, are shown in Figure 5.1. Note that stress intensities in most areas are low (less than 500 psi, or 5% of the most conservative critical stress). Peak stresses tend to occur on the outer bank hoods exposed to the main steam lines (MSLs), the adjacent reinforcement bars, and welds.

ANSYS provides nodal averaged values for stress components, which were used to derive stress intensity and alternating stress intensity, as described in Section 4.2. To yield the conservative estimate for nodal stresses at the weld locations, where several components are joined together, the stresses were computed by averaging element results on each component. Thus, for nodes at the weld locations several stress estimates were calculated each corresponding to a single component. All these stresses were then post-processed in order to determine the lowest stress ratios. No additional averaging was performed.

5.2 Maximum Stress Locations

The maximum stress intensities obtained from ANSYS are listed in Table 5.1. Note that these stress intensities *do not* account for weld factors. Further, it should be noted that since the allowable stresses vary with location, peak stress intensities do not necessarily correspond to regions of primary structural concern. Instead, structural evaluation is more accurately made in terms of the stress ratios which compare the computed stresses to allowable levels with due account made for stress type and weld factors. Comparisons on the basis of stress ratios is made in Table 6.3.

The tabulated stresses are obtained by computing the relevant stress intensities at every node and then sorting the nodes according to stress levels. The maximum stress node is noted and all neighboring nodes within 10" of the maximum stress node and its symmetric images (i.e., reflections across the x=0 and y=0 planes) are 'blanked' (i.e., excluded from the search for subsequent peak stress locations). Of the remaining nodes, the next highest stress node is identified and its neighbors (closer than 10") blanked. Finally the third highest stress node is located. The blanking of neighboring nodes is intended to prevent extracting peak stress nodes from essentially the same location on the structure.

The maximum membrane+bending (Pm+Pb) occur where the thin closure plate joins to the inner hood. The highest alternating (S_{alt}) stress intensities occur primarily on the outer hoods away from welds. This is also where the peak membrane stresses occurs. Contour plots of the peak and alternating stress intensities over the steam dryer structure are shown in Figures 5.2-5.4. The figures are oriented to emphasize the maximum stress.

Table 5.1. Locations with highest predicted stress intensities. Stresses are categorized according to stress type (membrane – Pm; membrane+bending – Pm+Pb and alternating – S_{alt}) and location (away from weld or at weld)

			Location (in)				Stress (psi)		
Stress Category	Location	Weld	x	y	z	node	Pm	Pm+Pb	S_{alt}
max. Pm	Trough thin section / trough bottom plate	Yes	-117.3	14.4	7.5	84611	6554	6755	367
"	Thin closure plate top/inner hood	Yes	108.4	-27.5	95.0	80900	6309	6718	852
"	Inner hood bottom/center support junction	Yes	-0.0	-38.4	7.5	83761	5637	5738	3038
"	Outer hood / end plate	Yes	68.1	101.4	7.5	58204	4315	4355	882
"	Thin closure plate bottom/inner hood near reinforcement	Yes	-108.4	38.5	9.0	80390	4294	4432	1145
max. Pm+Pb	Trough thin section / trough bottom plate	Yes	-117.3	14.4	7.5	84611	6554	6755	367
"	Thin closure plate top/inner hood	Yes	108.4	-27.5	95.0	80900	6309	6718	852
"	Inner hood bottom/center support junction	Yes	-0.0	-38.4	7.5	83761	5637	5738	3038
"	Thin closure plate bottom/inner hood near reinforcement	Yes	-108.4	38.5	9.0	80390	4294	4432	1145
"	Outer hood / end plate	Yes	68.1	101.4	7.5	58204	4315	4355	882
max. S_{alt}	Inner hood bottom/center support junction	Yes	-0.0	-38.4	7.5	83761	5637	5738	3038
"	Thin closure plate top/middle hood	Yes	84.7	-58.9	95.0	81905	3919	4217	2601
"	Outer hood, mid-height (side MSL CD)	No	-0.3	94.7	78.6	37726	344	2631	2531
"	Outer hood, lower-height (side MSL AB)	No	0.7	-101.3	26.6	38587	204	2625	2461
"	Drain cover/skirt (submerged)	Yes	118.1	-12.0	-94.3	23275	1749	3165	2444

Node numbers are retained for further reference. X-axis is parallel to the hoods, Y-axis is normal to the hoods, positive in direction from MSL AB to MSL CD, Z-axis is vertical, positive up. Origin is at the centerline of steam dryer 7.5" below bottom plates.

Thin closure plates - the 3/16 inch plates on the steam outlet side of the outer and middle vane banks. The straight vertical edge is welded to the vane bank end plate and on curved vertical edge is welded to the outside of the curved hood. These plates ensure that the steam exiting the vane banks is directed upward into the dome.

Thick closure plate - this 1/2 inch plate performs the same function as the thin closure plate, but it spans the steam outlet space between two inner hoods vane banks.

Supports - the vertical stiffeners on the inside of the hoods. The straight vertical edge is welded to the inlet of the vane bank assembly. The curved vertical edge is welded to the inside of the hood

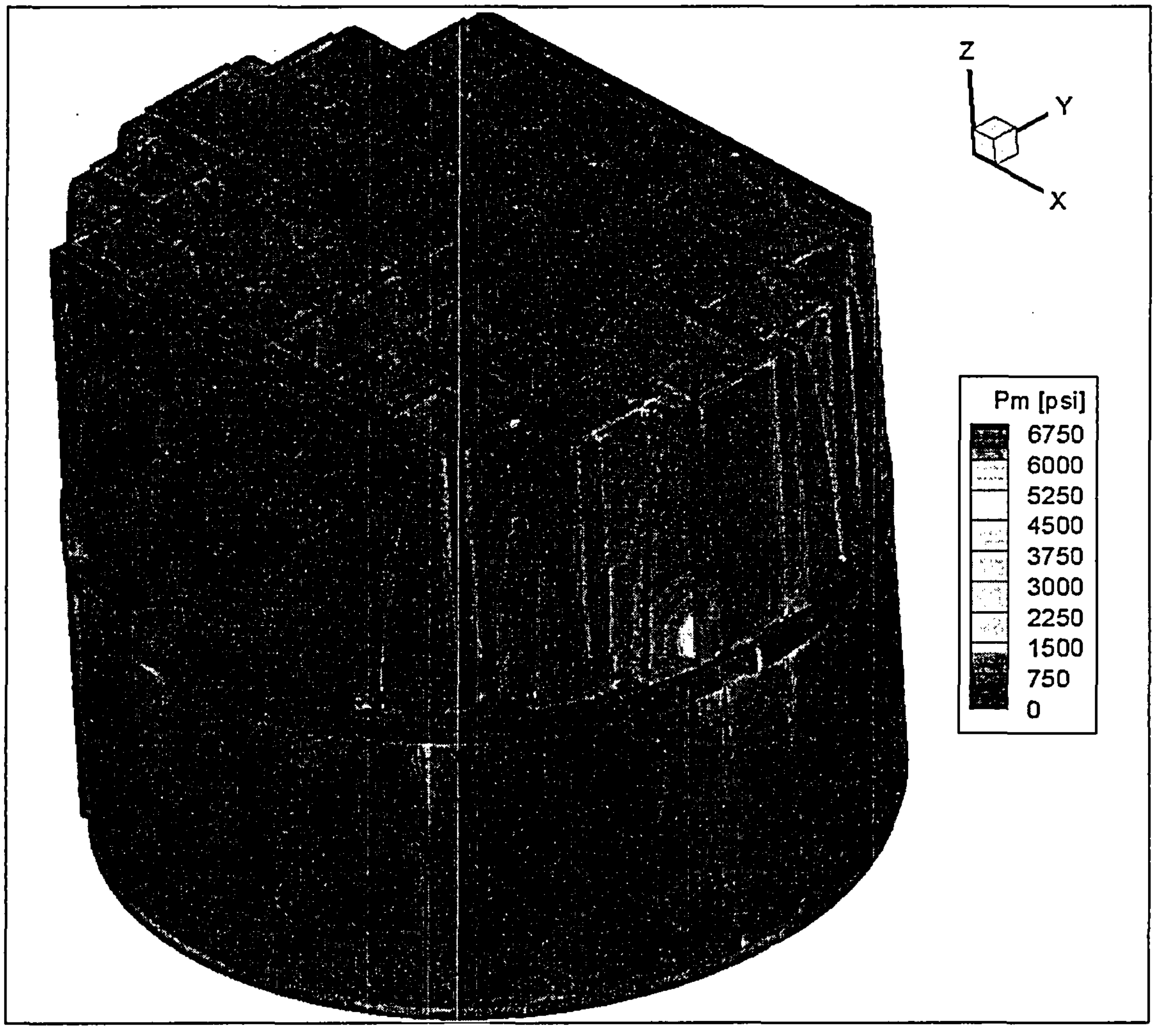

Figure 5.2. Contour plot of peak membrane stress intensity, Pm. The maximum stress intensity is 6554 psi.

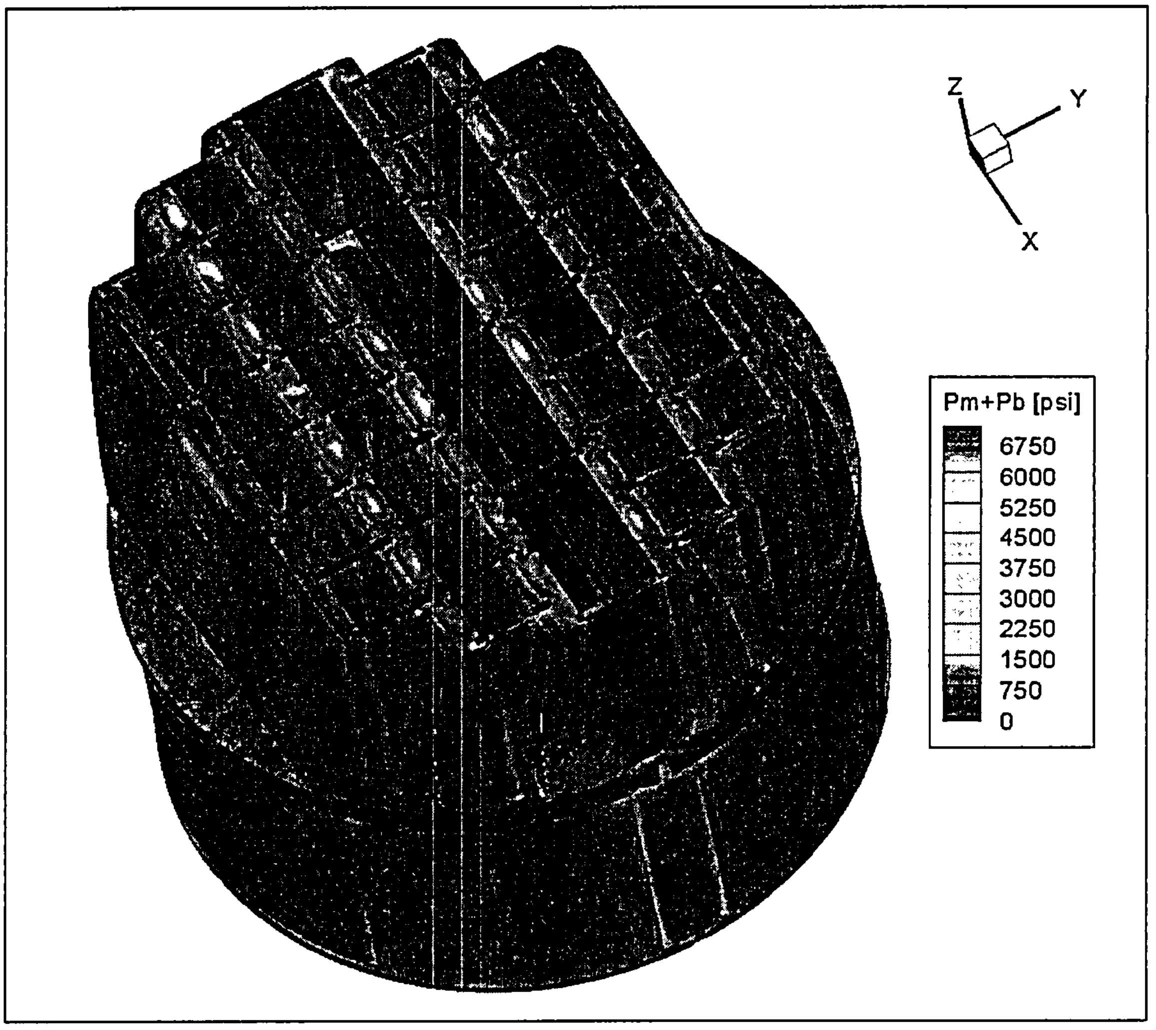

Figure 5.3. Contour plot of peak membrane+bending stress intensity, Pm+Pb. The maximum stress intensity is 6755 psi.

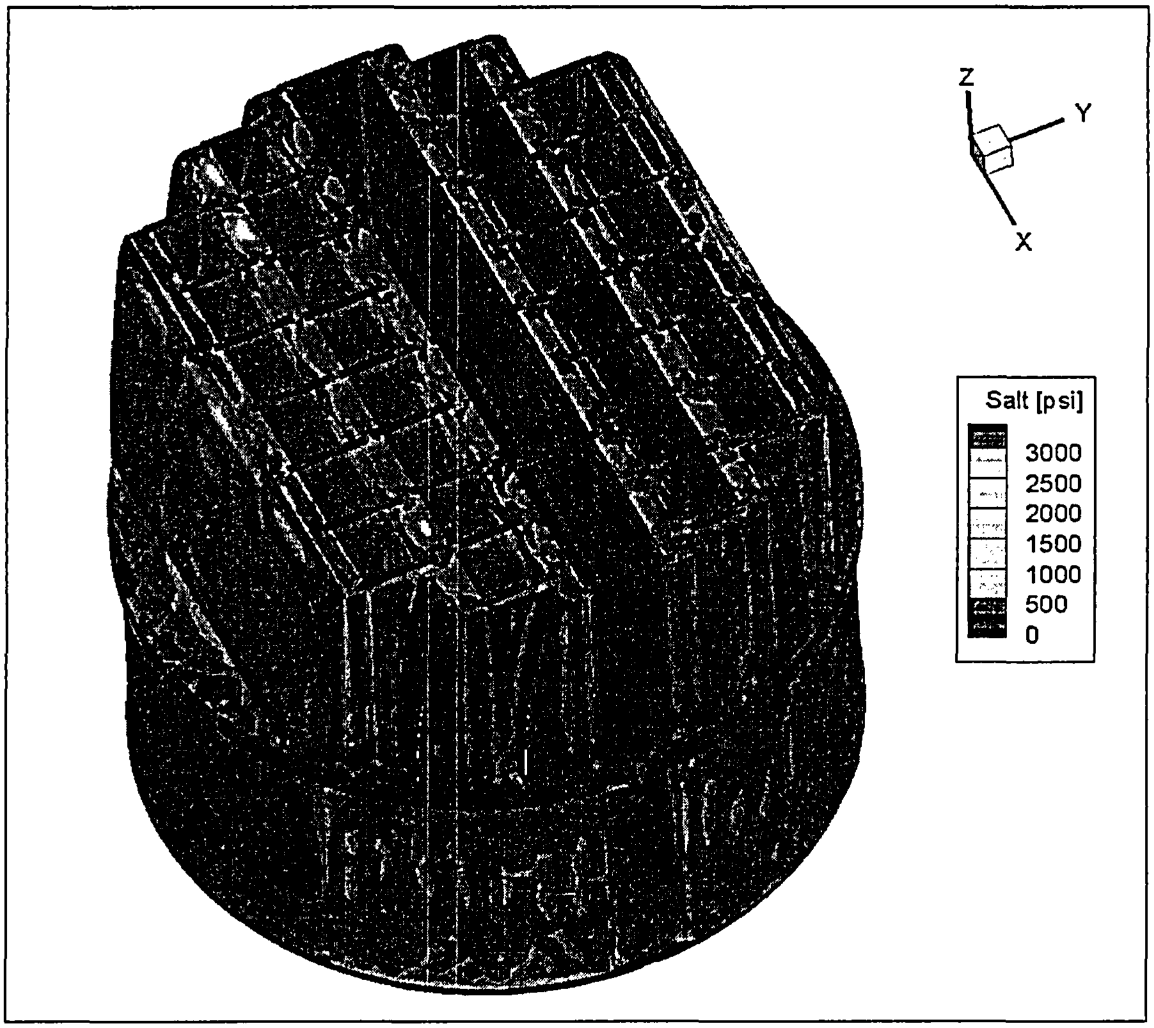

Figure 5.4. Contour plot of alternating stress intensity, S_{alt}. The maximum stress intensity is 3038 psi.

6. Load Combinations and Allowable Stress Intensities.

6.1 Load Combinations for Evaluation

The ASME B&PV Code, Section III, subsection NG provides different allowable stresses for different load combinations and plant conditions. The stress levels of interest in this analysis are for the normal operating condition, which is the Level A service condition. The load combination for this condition is:

Normal Operating Load Combination = Weight + Pressure + Thermal

The weight and fluctuating pressure contributions have been calculated in this analysis and are included in the stress results. The static pressure differences and thermal expansion stresses are small, since the entire steam dryer is suspended inside the reactor vessel and all surfaces are exposed to the same conditions.

Seismic loads only occur in Level B and C cases, and are not considered in this analysis.

6.2 Allowable Stress Intensities

The ASME B&PV Code, Section III, subsection NG shows the following (Table 6.1) for the maximum allowable stress intensity (Sm) and alternating stress intensity (Sa) for the Level A service condition. The allowable stress intensity values for type 304 stainless steel at operating temperature 550°F are taken from Table I-1.2 and Fig. I-9.2.2 of Appendix I of Section III, the ASME B&PV Code. The calculation for different stress categories is performed in accordance with Fig. NG-3221-1 of Division I, Section III, subsection NG.

Table 6.1. Maximum Allowable Stress Intensity and Alternating Stress Intensity for all areas other than welds. The notation Pm represents membrane stress; Pb represents stress due to bending; Q represents secondary stresses (from thermal effects and gross structural discontinuities, for example); and F represents peak stresses (due to local structural discontinuities, for example).

Type	Notation	Calculation	Allowable Value (psi)
	Peak Stress Allowables:		
General Membrane	Pm	Sm	18,300
Membrane + Bending	Pm + Pb	1.5 Sm	27,450
Primary + Secondary	Pm + Pb + Q	3.0 Sm	54,900
	Alternating Stress Allowable:		
Primary + Secondary + Peak	S_{alt}	Sa	13,600

When evaluating welds, either the calculated or allowable stress was adjusted, to account for a stress concentration factor. Specifically:

- For maximum allowable stress intensity, the allowable value is decreased by multiplying its value in Table 6.1 by 0.55.

- For alternating stress intensity, the calculated weld stress intensity is multiplied by a weld stress intensity (fatigue) factor of 1.8, before comparison to the Sa value given above.

The factors of 0.55 and 1.8 were selected based on the observable quality of the shop welds and NDE testing of all welds (excluding tack and intermittent welds) during fabrication. GE Purchase Specification for the HCGS Steam Dryer (21A9355 Section 9.2) called for liquid penetrant testing of all welds (excluding tack and intermittent welds) along the entire length or circumference, using the guidance of ASME Boiler and Pressure Code, Paragraph N-6127.3. In addition, critical welds are subject to periodical visual inspections in accordance with the requirements of GE SIL 644. Therefore, for weld stress intensities, the allowable values are shown in Table 6.2.

Table 6.2. Weld Stress Intensities.

Type	Notation	Calculation	Allowable Value (psi)
	Peak Stress Allowables:		
General Membrane	Pm	0.55 Sm	10,065
Membrane + Bending	Pm + Pb	0.825 Sm	15,098
Primary + Secondary	Pm + Pb + Q	1.65 Sm	30,195
	Alternating Stress Allowable:		
Primary + Secondary + Peak	S_{alt}	Sa	13,600

6.3 Comparison of Calculated and Allowable Stress Intensities

The classification of stresses into general membrane or membrane + bending types was made according to the exact location, where the stress intensity was calculated; namely, general membrane, Pm, for middle surface of shell element, and membrane + bending, Pm + Pb, for other locations. For solid elements the most conservative, general membrane, Pm, allowable is used.

The structural assessment is carried out by computing stress ratios between the computed peak and alternating stress intensities, and the allowable levels. Locations where any of the stress exceed allowable levels will have stress ratios less than unity. Since computation of stress ratios and related quantities within ANSYS is time-consuming and awkward, a separate FORTRAN code was written to compute the necessary peak and alternating stress intensities, Pm, Pm+Pb and S_{alt}, and then compare it to allowables. Specifically, the following quantities were computed at every node:

1. The peak membrane stress intensity, Pm (evaluated at the mid-thickness location for shells),
2. The peak stress intensity, Pm+Pb, (taken as the maximum of the peak stress intensity values at the bottom, top and mid thickness locations, for shells),

3. The peak alternating stress, S_{alt}, (the maximum value over the three thickness locations is taken).
4. The minimum peak stress ratio assuming the node lies at a non-weld location:
   SR-P(nw) = min{ Sm/Pm,   1.5 * Sm/(Pm+Pb) }.
5. The alternating stress ratio assuming the node lies at a non-weld location,
   SR-a(nw) = Sa / (1.1 * S_{alt}),
6. The same as 4, but assuming the node lies on a weld,
   SR-P(w)=SR-P(nw)*0.55.
7. The same as 5, but assuming the node lies on a weld,
   SR-a(w)=SR-a(nw)/1.8.

Note that in steps 4 and 6, the minimum of the stress ratios based on Pm and Pm+Pb, is taken. The allowables listed in Table 6.1, Sm=18,300 psi and Sa=13,600 psi. The factors, 0.55 and 1.8, are the weld factors discussed above. The factor of 1.1 accounts for the differences in Young's moduli for the steel used in the steam dryer and the values assumed in alternating stress allowable. According to NG-3222.4 the effect of elastic modulus upon alternating stresses is taken into account by multiplying alternating stress S_{alt} at all locations by the ratio, E/E_{model}=1.1, where:

$E = 28.3\ 10^6$ psi, as shown on Fig. I-9.2.2. ASME BP&V Code
$E_{model} = 25.55\ 10^6$ psi (Table 2.1)

The nodes with stress ratios exceeding 4 are plotted in TecPlot to establish whether they lie on a weld or not. The appropriate peak and alternating stress ratios, SR-P and SR-a, are thus determined and a final listing of nodes having minimum stress ratios is generated

Nodes identified as having the smallest stress ratios are listed below, in Table 6.3. . The corresponding locations are depicted in Figures 6.1. The minimum peak and alternating stress ratios at non-welds all exceed SR-P>3.5 and are not considered further. The minimum peak stress ratio at a weld is SR-P=1.54 and occurs on the trough along the junction of the vertical thin section and bottom plate. The smallest alternating stress ratio, SR-a=2.26, occurs at the weld along the junction of the inner hood and its support.

Table 6.3. Comparison of Calculated and Allowable Stress Intensities. Stress ratio is the ratio of allowable calculated stress intensity to calculated stress intensity. Bold text indicates minimum stress ratio. Note: At all non-weld locations, SR-P>3.5 and SR-a>4. Locations are depicted in Figure 6.1.

Stress Ratio	Location	Weld	Location (in)				Computed Stress Intensity (psi)				
			x	y	z	node	Pm	Pm+Pb	S_{alt}	SR-P	SR-a
SR-P	**1. Trough thin section / trough bottom plate**	**Yes**	**-117.3**	**14.4**	**7.5**	**84611**	**6554**	**6755**	**6554**	**1.54**	**18.7**
"	2. Thin closure plate top/inner hood	"	108.4	-27.5	95.0	80900	6309	6718	6309	1.60	8.06
"	3. Inner hood bottom/center support junction	"	0.0	-38.4	7.5	83761	5637	5738	5637	1.79	2.26
"	4. Outer hood / end plate	"	68.1	101.4	7.5	58204	4315	4355	4315	2.33	7.78
SR-a	1. Inner hood bottom/center support junction	Yes	0.0	-38.4	7.5	83761	5637	5738	5637	1.79	2.26
"	2. Thin closure plate top/middle hood	"	84.7	-58.9	95.0	81905	3919	4217	3919	2.57	2.64
"	3. Drain cover/skirt (submerged)	"	118.1	-12.0	-94.3	23275	1749	3165	1749	4.77	2.81
"	4. Outer hood (bottom) / cover plate	"	1.8	-101.5	7.5	35750	1816	2931	1816	5.15	3.25

Stress ratios are calculated using stress allowables according to Tables 6.1 and 6.2. The tabulated alternating stresses, S_{alt}, are taken from the ANSYS computation and do not reflect adjustments at welds. However, the computed alternating stresses are corrected by a factor 1.1 everywhere (Young's modulus adjustment), and a weld factor of 1.8 at weld locations before evaluating stress ratios.

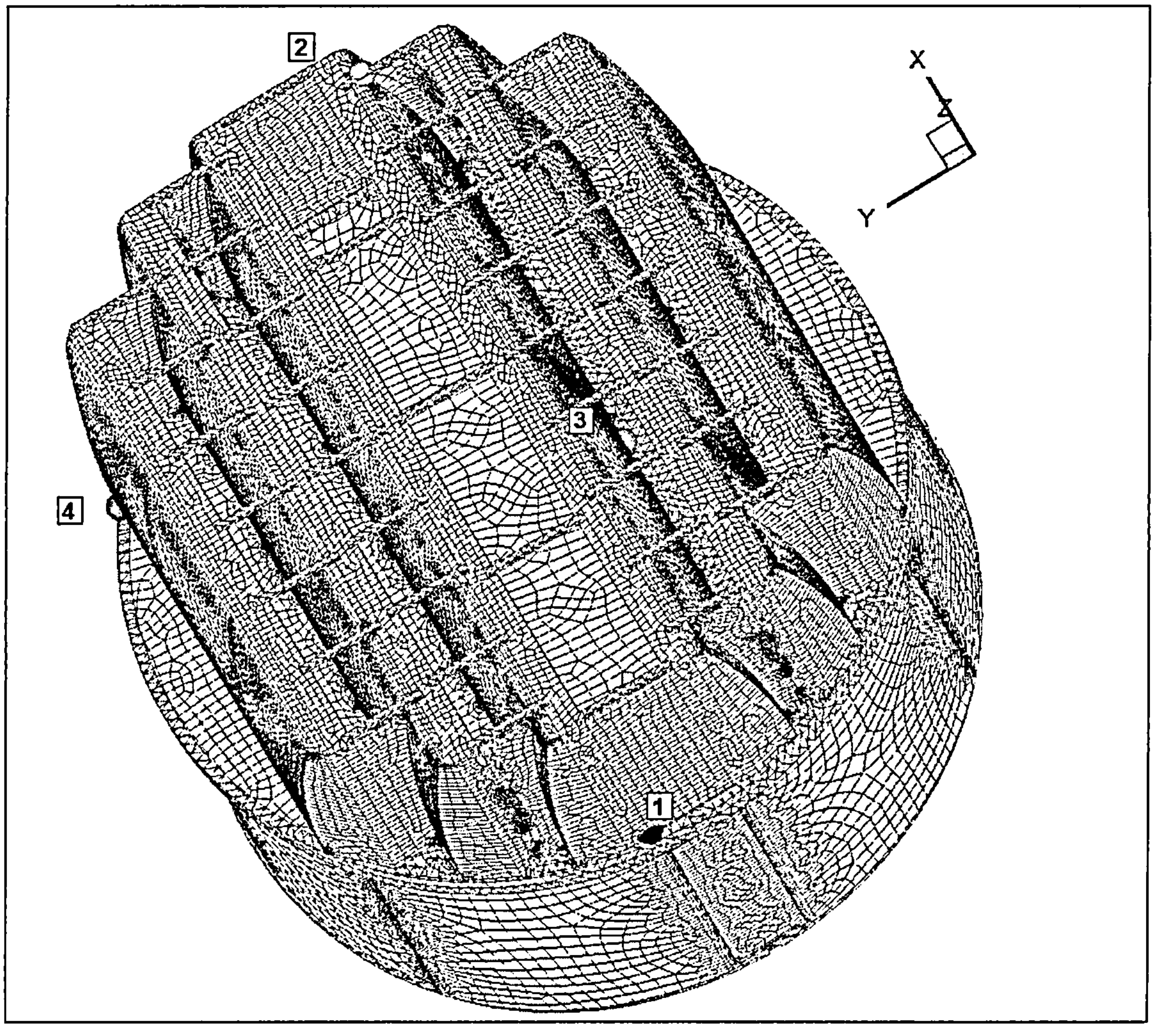

Figure 6.1a Locations of minimum peak stress ratios, SR-P, at welds.

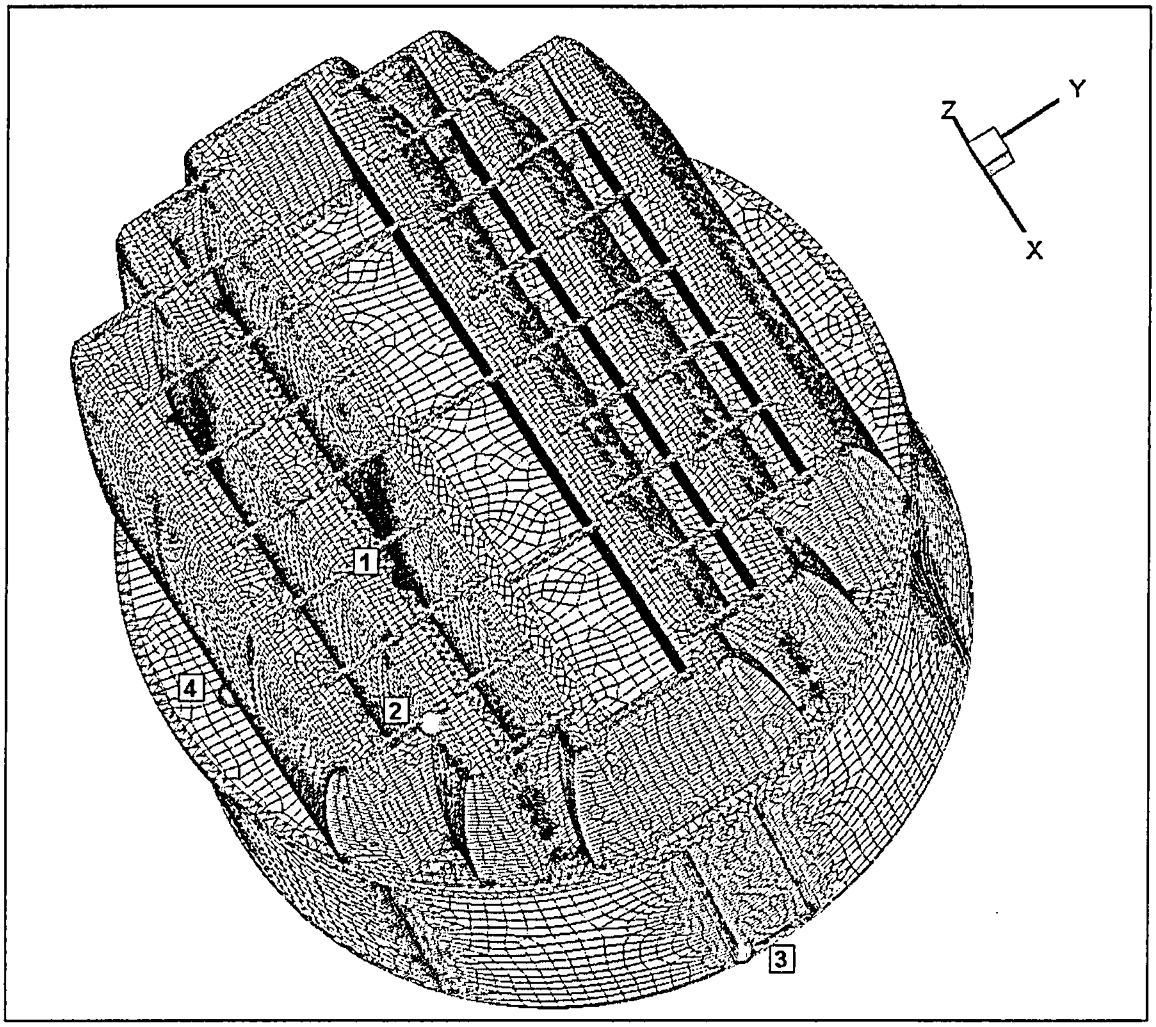

Figure 6.1b Locations of minimum alternating stress ratios, SR-a, at welds.

6.4 PSD of Stress Time History at Outer Hood Supports

Stress intensities are found to be high on the outer hoods and it is useful to examine the power spectral density of the maximum component of the stress at these locations. Figure 6.1 compares the PSDs of the stress histories on the outer hoods near the MSLs. The stress PSDs are somewhat noisier than those from the loads because of the lower number of samples (300 time steps). The PSDs on both the AB and CD MSLs are in close agreement. Both display prominent peaks at about 48Hz, 58 Hz, 80Hz and 119 Hz and troughs at about 68Hz, 108Hz and 145Hz.

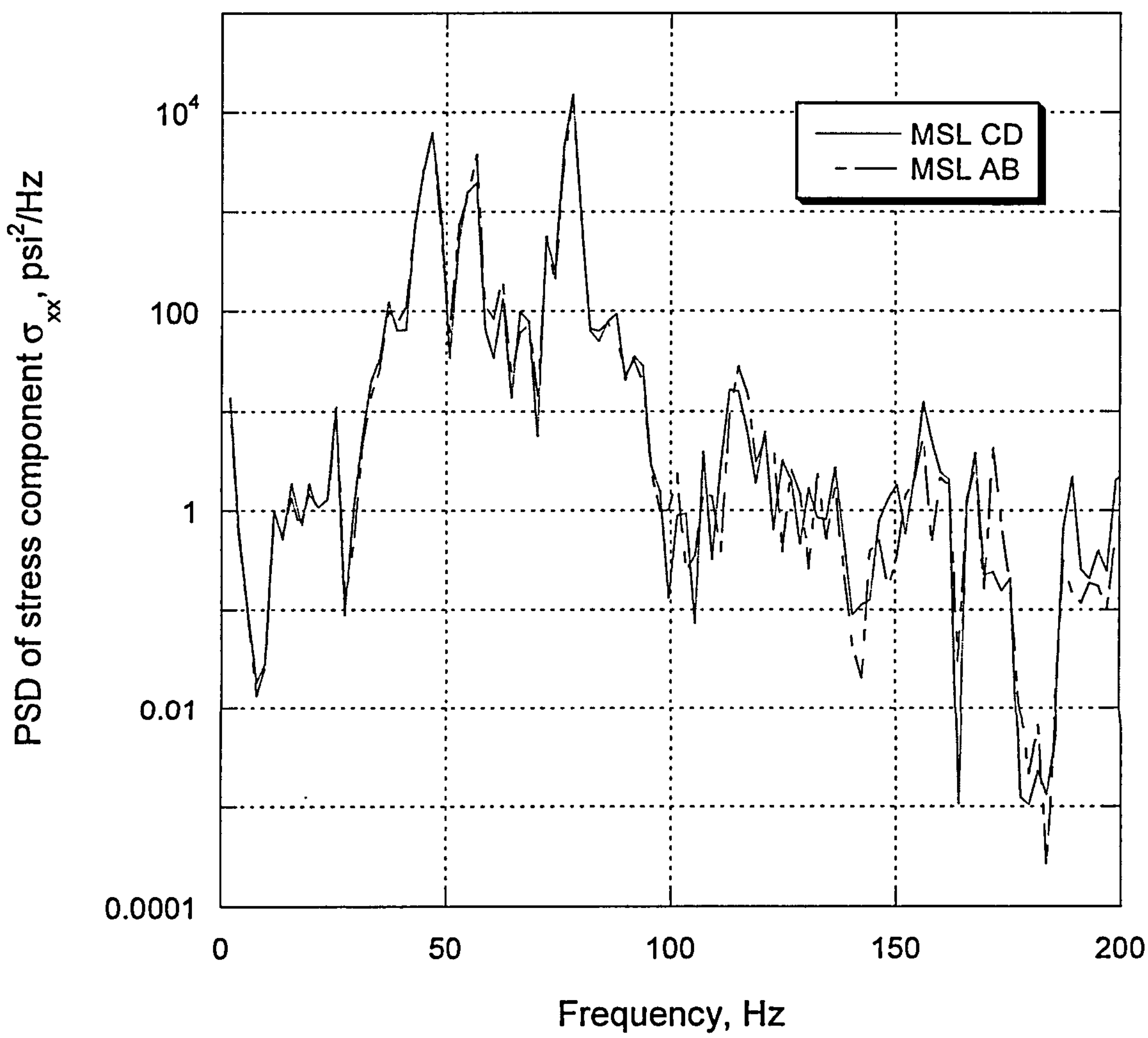

Figure 6.1. PSD of pressure load and stress, σ_{xx}, on outer hood supports, where the x direction points horizontally and tangential to the hood surface.

7. Conclusions

The dynamic analysis of the steam dryer at Hope Creek Unit 1 shows that the steam flow and gravity loads produce stresses that meet all of the allowable stress values of the ASME, B&PV Code, Section III, subsection NG. Since these loads represent practically the full load condition for normal operation (Level A Service Level), we conclude that the steam dryer will continue to operate without structural failure.

Maximum points of stress and the calculated / allowable stress ratios are tabulated in Section 6 of this report. This tabulation shows a minimum stress ratio of 1.54. All other locations on the steam dryer have significantly lower stresses than those listed in Section 6.

It is important to recognize that the results presented above <u>do not</u> account for any factors of conservatism and uncertainty in the applied loads. It is expected that when all factors are accounted for that the stress ratios will increase significantly so that all minimum stress ratios will be well within allowables.

8. References

1. Continuum Dynamics, Inc. 2006. Hydrodynamic Loads on Hope Creek Unit 1 Steam Dryer C.D.I. Report No. 06-17 (to be issued).

2. Meijers, P. 1985. Refined Theory for Bending and Torsion of Perforated Plates. *Journal of Pressure Vessel Technology* 108: 423-429.

3. Continuum Dynamics, Inc. August 2006. High and Low Frequency Steam Dryer Loads by Acoustic Circuit Methodology. C.D.I. Technical Memorandum No. 06-25P.